

HCV genome replication by interaction with NS5A. Hsp90 is a molecular chaperone that is highly expressed in most cell types in various organisms (Neckers, 2002). Here, Hsp90 was found to be able to bind to FKBP8 and form a complex with HCV NS5A. The suppression of NS5A, but not that of FKBP8, was observed in replicon cells treated with geldanamycin, thus suggesting that Hsp90 regulates the replication of HCV RNA via the interaction with FKBP8. It is well known that several host proteins such as VAPs and FBL2 interact with the HCV replication complex and regulate HCV RNA replication (Evans *et al*, 2004; Gao *et al*, 2004; Hamamoto *et al*, 2005; Wang *et al*, 2005). The TPR domain of FKBP8 is composed of 220 amino acids and is too long to determine the critical residues responsible for interaction with NS5A. Therefore, we tried to make a chimeric mutant carrying the TPR of FKBP52 to determine the critical amino-acid residues for binding to NS5A in FKBP8. However, expression of a chimeric FKBP8 possessing TPR of FKBP52 was much lower than the native form, suggesting that TPR domain is critical for stability and conformation of FKBP8. Amino-acid residues responsible for the binding to NS5A must be different from the two-carboxylate positions responsible for Hsp90 binding and locate within the TPR domain. The ternary complex consists of NS5A, FKBP8 and Hsp90 may be involved in the replication of HCV. FKBP52 possesses PPIase activity and chaperone activity in domain I (amino acids 1–148) and domain 3 (TPR domain, amino acids 264–400), respectively (Pirkl *et al*, 2001). Therefore, it is reasonable to speculate that the TPR domain is responsible for the chaperone activity of FKBP8, and that the FKBP8 and NS5A complex transports Hsp90 to the appropriate clients, including viral and host proteins, which in turn leads to the stabilization of the replication complex and the enhancement of HCV RNA replication.

In this study, we identified human FKBP8 as a binding partner of HCV NS5A. Our results suggest that the interaction between FKBP8 and HCV NS5A is essential for HCV replication. The NS5A protein forms a complex with FKBP8 and Hsp90, and an inhibitor of Hsp90 was shown to reduce the efficiency of HCV replication. The elucidation of the molecular mechanisms underlying the formation of the NS5A/FKBP8/Hsp90 complex may lead to the development of new therapeutics for chronic hepatitis C.

## Materials and methods

### Yeast two-hybrid assays

Screening for the gene-encoding host protein that interacts with HCV NS5A was performed with a yeast two-hybrid system, Matchmaker two-hybrid system 3 (Clontech, Palo Alto, CA), according to the manufacturer's protocol. Human fetal brain and liver libraries were purchased from Clontech. The cDNA of NS5A-encoding amino acids 1973–2419 of an HCV polyprotein of the J1 strain (genotype 1b) (Aizaki *et al*, 1998) was amplified by PCR and was cloned into the pGBKT7 vector (Clontech) (Tu *et al*, 1999; Hamamoto *et al*, 2005).

### Plasmids

DNA fragments encoding NS5A were amplified from HCV genotype 1b strains J1 and Con1 (provided by Dr Bartenschlager), genotype 1a strain H77C (provided by Dr Bukh), and genotype 2a strain JFH-1 (provided by Dr Wakita) by PCR using *Pfu* turbo DNA polymerase (Stratagene, La Jolla, CA). The fragments were cloned into pCAGGs-PUR/N-HA, in which the sequence encoding an HA tag is inserted at the 5'-terminus of the cloning site of pCAGGs-PUR (Niwa *et al*, 1991). The DNA fragment encoding human FKBP8 was amplified from the total cDNA of Huh7 cells by PCR, and this

fragment was introduced into pEF-FLAG pGBK puro (Huang *et al*, 1997), pCAGGs-PUR/NHA, pcDNA3.1-N-HA (Tu *et al*, 1999; Hamamoto *et al*, 2005), and pcDNA3.1-N-EE, in which an Glu-Glu (EE) tag is inserted in the 5'-terminus of the cloning site of pcDNA3.1 (+) (Invitrogen, Carlsbad, CA). The DNA fragments encoding human Hsp90, FKBP52, and CypD were amplified from a human fetal brain library (Clontech) by PCR, and were introduced into pcDNA3.1-N-HA. The genes encoding the deletion mutants of human FKBP8 were amplified and cloned into pCAGGs-PUR/NHA. The gene encoding an FKBP8 mutant replaced Lys<sup>307</sup> and Arg<sup>311</sup> with Ala, designated as FKBP8TPRmut, was generated by the method of splicing by overlap extension and introduced into pEF-Flag pGBKpuro. The gene encoding an Hsp90 mutant lacking the C-terminal MEEVD motif of Hsp90, designated as Hsp90ΔMEEVD, was amplified and cloned into pcDNA3.1-N-HA. All PCR products were confirmed by sequencing by an ABI PRISM 310 genetic analyzer (Applied Biosystems, Tokyo, Japan).

### Cell lines

Human embryonic kidney 293T cells and the human hepatoma cell lines Huh7 and FLC-4 were maintained in Dulbecco's modified Eagle's medium (DMEM) (Sigma, St Louis, MO) containing 10% fetal calf serum (FCS), whereas the Huh 9–13 cell line, which possesses an HCV subgenomic replicon (Lohmann *et al*, 1999), was cultured in DMEM supplemented with 10% FCS and 1 mg/ml G418. All cells were cultured at 37°C in a humidified atmosphere with 5% CO<sub>2</sub>.

### Antibodies

Mouse monoclonal antibodies to the HA and EE tags were purchased from Covance (Richmond, CA). Anti-Flag mouse antibody M2, horseradish peroxidase-conjugated M2 antibody, and anti-β-actin mouse monoclonal antibody were purchased from Sigma. Mouse monoclonal antibody to NS5A was from Austral Biologicals (San Ramon, CA). Mouse monoclonal antibodies to NS4B and NS5B have been described previously (Kashiwagi *et al*, 2002). Rabbit polyclonal antibody to NS5A was prepared as described previously (Hamamoto *et al*, 2005). Rabbit polyclonal antibody to thioredoxin was described previously (Moriishi *et al*, 1999).

### Transfection, immunoblotting, and immunoprecipitation

The transfection and immunoprecipitation test were carried out by a previously described method (Hamamoto *et al*, 2005). The immunoprecipitates boiled in the loading buffer were subjected to 12.5% SDS-PAGE. The proteins were transferred to polyvinylidene difluoride membranes (Millipore, Bedford, MA) and were reacted with the appropriate antibodies. The immune complexes were visualized with Super Signal West Femto substrate (Pierce, Rockford, IL) and they were detected by an LAS-3000 image analyzer system (Fujifilm, Tokyo, Japan). The density of protein band was determined by using IMAGE-PRO PLUS 5.1 software (Media Cybernetics, Silver Springs, MD).

### Gene silencing by siRNA

The siRNA targeted to FKBP8, Target-1: 5'-GAGUGGCCUGGACAUC UGG-3', and negative control siRNA, that is, siCONTROL Non-Targeting siRNA-2, were purchased from Dharmacon (Lafayette, CO). Target-2, 5'-UCCCAUGGAAGUGGCUGUU-3', and Target-3, 5'-GACAACAUCAAGGCUCUCU-3' were purchased from Qiagen (Tokyo, Japan). The Huh7 cells harboring a subgenomic HCV replicon grown on six-well plates were transfected with 80 or 160 nM of siRNA with siFECTOR (B-Bridge International, Sunnyvale, CA). The cells were grown in DMEM containing 10% FCS and were then harvested at 48 or 72 h post-transfection.

### Real-time PCR

Total RNA was prepared from cell lines by using RNeasy mini kit (Qiagen). First-strand cDNA was synthesized by using a first-strand cDNA synthesis kit (Amersham Pharmacia Biotech, Franklin Lakes, NJ) and random primers. Each cDNA was estimated by Platinum SYBR Green qPCR SuperMix UDG (Invitrogen) according to the manufacturer's protocol. Fluorescent signals were analyzed by an ABI PRISM 7000 (Applied Biosystems). The HCV NS5A, human β-actin, and human FKBP8 genes were amplified using the primer pairs of 5'-AGTCAGTGTCTGCGCTTTC-3' and 5'-CGGGGAATTCCTGCTTC-3',

5'-TGGAGTCTGTGGCATCCACGAACTACCTTCAACTC-3'  
and 5'-CGGACTCGTCATACCTCTGCTTGCTGATCCACATC-3',  
and 5'-GGCTGTTGAGGAAGAAGACG-3'  
and 5'-CTTGGAGTCAGCACTGACCA-3', respectively. The FKBP8  
primers are located at different exons in order to prevent the  
false-positive amplification of contaminated genomic DNA. The  
values of the HCV genome and FKBP8 mRNA were normalized  
with those of  $\beta$ -actin mRNA. Each PCR product was detected as a  
single band of the correct size upon agarose gel electrophoresis  
(data not shown).

#### Establishment of cell lines expressing an siRNA-resistant FKBP8 mutant and knockdown FKBP8 expression

A, G, and T at nucleotides 273, 276, and 288 from the 5' end of the  
open-reading frame of human FKBP8 were replaced with G, A, and  
C, respectively, according to a splicing method achieved by overlap  
extension; these silent mutations were then cloned into pEF-Flag  
pGBKpuro. The resulting plasmid encoding a mutant FKBP8  
resistant to knockdown by siRNA was transfected into Huh7 cells  
harboring the HCV RNA replicon. The culture medium was replaced  
with DMEM supplemented with 10% FCS and 2  $\mu$ g/ml of puromycin  
(Nakarai Tesque, Tokyo, Japan) at 24 h post-transfection, and the  
cells were cultured for 7 days. The surviving cells were used for the  
FKBP8 knockdown experiments. The shRNAs targeted to FKBP8,  
the target sequences of which were 5'-GATCCGCTGGAACCTTCCA  
ACAAGTTCAAGAGACTTGTGGAAAGGTTCCAGCTTA-3', and 5'-A  
GCTTAAGCTGGAACCTTCCAACAAGTCTTGAAGTCTTGGAAAGG  
TTCCAGCG-3', were annealed and introduced between the *Bam*HI  
and *Hind*III sites of pSilencer<sup>TM</sup> 2.1-U6 hygro (Ambion, Austin, TX)  
according to the manufacturer's protocol. An HCV replicon cell line  
cured with IFN- $\alpha$  was transfected with 5  $\mu$ g of the plasmid by  
electroporation. The culture medium was replaced with DMEM  
supplemented with 10% FCS and 500  $\mu$ g/ml of Hygromycin B  
(Wako, Tokyo, Japan) at 24 h post-transfection. The remaining cells  
were re-seeded in 98-well plates and cloned for the colony  
formation and transient replication assays.

#### Colony formation assay

The plasmid pFK-I<sub>389</sub> neo/NS3-3'/NK5.1 (Pietschmann *et al*, 2002)  
was obtained from R Bartenschlager. The plasmid cleaved at the  
*Scal* site was transcribed *in vitro* using the MEGAscript T7 kit  
(Ambion) according to the manufacturer's protocol. The linearized  
plasmid (10  $\mu$ g) was introduced into Huh7 cells at 4 million cells/  
0.4 ml by electroporation at 270 V and 960  $\mu$ F using a Gene Pulser<sup>TM</sup>  
(Bio-Rad, Hercules, CA). Electroporated cells were suspended at a  
final volume of 10 ml of culture medium. Three-milliliter aliquots  
of cell suspension were mixed with 7 ml of culture medium and  
then the cells were seeded on culture dishes (diameter: 10 cm). The  
culture medium was replaced with DMEM containing 10% FCS  
and 1 mg/ml of G418 (Nakarai Tesque) at 24 h post-transfection.  
The medium was exchanged weekly for fresh DMEM containing  
10% FCS and 1 mg/ml G418. The remaining colonies were fixed  
with 4% paraformaldehyde at 4 weeks after electroporation, and  
the cells were stained with crystal violet.

## References

Aizaki H, Aoki Y, Harada T, Ishii K, Suzuki T, Nagamori S, Toda G,  
Matsuura Y, Miyamura T (1998) Full-length complementary DNA  
of hepatitis C virus genome from an infectious blood sample.  
*Hepatology* 27: 621-627  
Appel N, Pietschmann T, Bartenschlager R (2005) Mutational  
analysis of hepatitis C virus nonstructural protein 5A: potential  
role of differential phosphorylation in RNA replication and iden-  
tification of a genetically flexible domain. *J Virol* 79: 3187-3194  
Boguski MS, Sikorski RS, Hieter P, Goebel M (1990) Expanding  
family. *Nature* 346: 114  
Brinker A, Scheufler C, Von Der Mulbe F, Fleckenstein B, Herrmann  
C, Jung G, Moarefi I, Hartl FU (2002) Ligand discrimination by  
TPR domains. Relevance and selectivity of EEVD-recognition in  
Hsp70 Hop Hsp90 complexes. *J Biol Chem* 277: 19265-19275  
Chadli A, Bouhouche I, Sullivan W, Stensgard B, McMahon N,  
Catelli MG, Toft DO (2000) Dimerization and N-terminal domain  
proximity underlie the function of the molecular chaperone heat  
shock protein 90. *Proc Natl Acad Sci USA* 97: 12524-12529

#### Transient replication assay

The cDNA encoding *Renilla* luciferase was introduced between the  
*AscI* and *PmeI* sites of the plasmid pFK-I<sub>389</sub> neo/NS3-3'/NK5.1, in  
place of the *neo* gene. The resulting plasmid, pFK-I<sub>389</sub> hRL/NS3-3'/  
NK5.1, was cleaved with *Scal* and was transcribed *in vitro* using  
a MEGAscript T7 kit (Ambion). Huh7 cells were suspended at 10  
million cells/ml and the suspensions were mixed with 10  $\mu$ g of  
*in vitro*-transcribed RNA at a 400- $\mu$ l volume; the cells were then  
electroporated at 270 V and 960  $\mu$ F by a Gene Pulser<sup>TM</sup> (Bio-Rad).  
The electroporated cells were suspended in 25 ml of culture medium  
and then were seeded at 1 ml/well on 12-well culture plates.  
Luciferase activity was measured at 4 and 48 h post-transfection  
using a *Renilla* Luciferase assay system (Promega, Madison, WI)  
according to the manufacturer's protocol. Luciferase activity at 4 h  
after electroporation was used to determine the transfection  
efficiency.

#### Generation of infectious HCV particles

The viral RNA of JFH1 was introduced into Huh7.5.1 according to  
the method of Wakita *et al* (2005). The supernatant was collected  
at 7 days post-transfection and used as HCV particles that are  
infectious in cell culture (HCVcc). The naïve Huh7.5.1 cells  
were transfected with siRNA of nontarget control or FKBP8-Target  
1 at a concentration of 80 nM. The siRNA-treated Huh7.5.1 cells  
were inoculated with HCVcc at 24 h post-transfection. Infected cells  
and culture supernatants were harvested every day until 5 days  
post-infection.

#### Determination of FKBP8-binding proteins

MEF purification was carried out by a previously described method  
(Ichimura *et al*, 2005). The FKBP8 gene was amplified by PCR and  
introduced into pcDNA3.1 encoding the myc-TEV-Flag epitope tag  
(Ichimura *et al*, 2005). The resulting plasmid was transfected into  
293T cells, which were then subjected to MEF purification. FKBP8-  
binding proteins were separated by SDS-PAGE and visualized by  
silver staining. The stained bands were excised, digested in gels  
with Lys-C, and analyzed by the direct nanoflow LC-MS/MS system  
(Ichimura *et al*, 2005).

#### Supplementary data

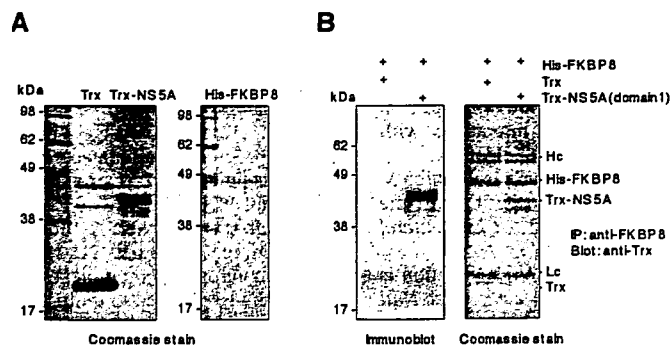
Supplementary data are available at *The EMBO Journal* Online  
(<http://www.embojournal.org>).

## Acknowledgements

We thank H Murase for secretarial work and H Miyamoto for  
discussion. We are also grateful to J Bukh, R Bartenschlager, and  
T Wakita for providing the HCV cDNAs and DCS Huang for the pEF-  
FLAG pGBK puro. This work was supported in part by grants-in-aid  
from the Ministry of Health, Labor, and Welfare; the Ministry of  
Education, Culture, Sports, Science, and Technology; the 21st  
Century Center of Excellence Program; and the Foundation for  
Biomedical Research and Innovation.

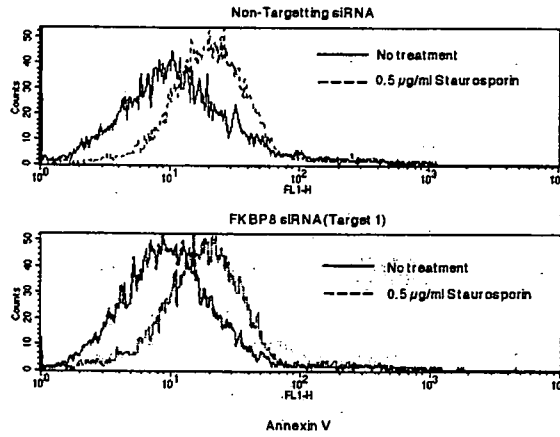
Cliff MJ, Harris R, Barford D, Ladbury JE, Williams MA (2006)  
Conformational diversity in the TPR domain-mediated interaction  
of protein phosphatase 5 with Hsp90. *Structure* 14: 415-426  
Edlich F, Weiwad M, Erdmann F, Fanghanel J, Jarczowski F, Rahfeld  
JU, Fischer G (2005) Bcl-2 regulator FKBP38 is activated by  
Ca(2+)/calmodulin. *EMBO J* 24: 2688-2699  
Evans MJ, Rice CM, Goff SP (2004) Phosphorylation of hepatitis C  
virus nonstructural protein 5A modulates its protein inter-  
actions and viral RNA replication. *Proc Natl Acad Sci USA* 101:  
13038-13043  
Fischer G, Aumuller T (2003) Regulation of peptide bond *cis/trans*  
isomerization by enzyme catalysis and its implication in  
physiological processes. *Rev Physiol Biochem Pharmacol* 148:  
105-150  
Gao L, Aizaki H, He JW, Lai MM (2004) Interactions between viral  
nonstructural proteins and host protein hVAP-33 mediate the  
formation of hepatitis C virus RNA replication complex on lipid  
raft. *J Virol* 78: 3480-3488

- Hamamoto I, Nishimune Y, Okamoto T, Aizaki H, Lee K, Mori Y, Abe T, Lai MC, Miyamura T, Moriishi K, Matsuura Y (2005) Human VAP-B is involved in HCV replication through interaction with NS5A and NS5B. *J Virol* 79: 13473–13482
- Hirano T, Kinoshita N, Morikawa K, Yanagida M (1990) Snap helix with knob and hole: essential repeats in *S. pombe* nuclear protein nuc2+. *Cell* 60: 319–328
- Huang DC, Cory S, Strasser A (1997) Bcl-2, Bcl-XL and adenovirus protein E1B19kD are functionally equivalent in their ability to inhibit cell death. *Oncogene* 14: 405–414
- Ichimura T, Yamamura H, Sasamoto K, Tominaga Y, Taoka M, Kakiuchi K, Shinkawa T, Takahashi N, Shimada S, Isobe T (2005) 14-3-3 proteins modulate the expression of epithelial Na<sup>+</sup> channels by phosphorylation-dependent interaction with Nedd4-2 ubiquitin ligase. *J Biol Chem* 280: 13187–13194
- Inoue K, Sekiyama K, Yamada M, Watanabe T, Yasuda H, Yoshida M (2003) Combined interferon alpha2b and cyclosporin A in the treatment of chronic hepatitis C: controlled trial. *J Gastroenterol* 38: 567–572
- Kapadia SB, Chisari FV (2005) Hepatitis C virus RNA replication is regulated by host geranylgeranylation and fatty acids. *Proc Natl Acad Sci USA* 102: 2561–2566
- Kashiwagi T, Hara K, Kohara M, Iwahashi J, Hamada N, Honda-Yoshino H, Toyoda T (2002) Promoter/origin structure of the complementary strand of hepatitis C virus genome. *J Biol Chem* 277: 28700–28705
- Koch JO, Bartenschlager R (1999) Modulation of hepatitis C virus NS5A hyperphosphorylation by nonstructural proteins NS3, NS4A, and NS4B. *J Virol* 73: 7138–7146
- Lackner T, Muller A, Konig M, Thiel HJ, Tautz N (2005) Persistence of bovine viral diarrhoea virus is determined by a cellular cofactor of a viral autoprotease. *J Virol* 79: 9746–9755
- Lam E, Martin M, Wiederrecht G (1995) Isolation of a cDNA encoding a novel human FK506-binding protein homolog containing leucine zipper and tetratricopeptide repeat motifs. *Gene* 160: 297–302
- Lindenbach BD, Evans MJ, Syder AJ, Wolk B, Tellinghuisen TL, Liu CC, Maruyama T, Hynes RO, Burton DR, McKeating JA, Rice CM (2005) Complete replication of hepatitis C virus in cell culture. *Science* 309: 623–626
- Lohmann V, Korner F, Koch J, Herian U, Theilmann L, Bartenschlager R (1999) Replication of subgenomic hepatitis C virus RNAs in a hepatoma cell line. *Science* 285: 110–113
- Macdonald A, Harris M (2004) Hepatitis C virus NS5A: tales of a promiscuous protein. *J Gen Virol* 85: 2485–2502
- Maggioli C, Braakman I (2005) Synthesis and quality control of viral membrane proteins. *Curr Top Microbiol Immunol* 285: 175–198
- Manns MP, McHutchison JG, Gordon SC, Rustgi VK, Shiffman M, Reindollar R, Goodman ZD, Koury K, Ling M, Albrecht JK (2001) Peginterferon alfa-2b plus ribavirin compared with interferon alfa-2b plus ribavirin for initial treatment of chronic hepatitis C: a randomised trial. *Lancet* 358: 958–965
- Mayer MP (2005) Recruitment of Hsp70 chaperones: a crucial part of viral survival strategies. *Rev Physiol Biochem Pharmacol* 153: 1–46
- Moriishi K, Inoue S, Koura M, Amano F (1999) Inhibition of listeriolysin O-induced hemolysis by bovine lactoferrin. *Biol Pharm Bull* 22: 1167–1172
- Moriishi K, Matsuura Y (2003) Mechanisms of hepatitis C virus infection. *Antivir Chem Chemother* 14: 285–297
- Nakagawa M, Sakamoto N, Tanabe Y, Koyama T, Itsui Y, Takeda Y, Chen CH, Kakinuma S, Oooka S, Maekawa S, Enomoto N, Watanabe M (2005) Suppression of hepatitis C virus replication by cyclosporin A is mediated by blockade of cyclophilins. *Gastroenterology* 129: 1031–1041
- Neckers L (2002) Hsp90 inhibitors as novel cancer chemotherapeutic agents. *Trends Mol Med* 8: S55–S61
- Neddermann P, Clementi A, De Francesco R (1999) Hyperphosphorylation of the hepatitis C virus NS5A protein requires an active NS3 protease, NS4A, NS4B, and NS5A encoded on the same polyprotein. *J Virol* 73: 9984–9991
- Nielsen JV, Mitchelmore C, Pedersen KM, Kjaerulf KM, Finsen B, Jensen NA (2004) Fkbp8: novel isoforms, genomic organization, and characterization of a forebrain promoter in transgenic mice. *Genomics* 83: 181–192
- Niwa H, Yamamura K, Miyazaki J (1991) Efficient selection for high-expression transfectants with a novel eukaryotic vector. *Gene* 108: 193–199
- Pietschmann T, Lohmann V, Kaul A, Krieger N, Rinck G, Rutter G, Strand D, Bartenschlager R (2002) Persistent and transient replication of full-length hepatitis C virus genomes in cell culture. *J Virol* 76: 4008–4021
- Pietschmann T, Lohmann V, Rutter G, Kurpanek K, Bartenschlager R (2001) Characterization of cell lines carrying self-replicating hepatitis C virus RNAs. *J Virol* 75: 1252–1264
- Pirkil F, Fischer E, Modrow S, Buchner J (2001) Localization of the chaperone domain of FKBP52. *J Biol Chem* 276: 37034–37041
- Qing K, Hansen J, Weigel-Kelley KA, Tan M, Zhou S, Srivastava A (2001) Adeno-associated virus type 2-mediated gene transfer: role of cellular FKBP52 protein in transgene expression. *J Virol* 75: 8968–8976
- Scheufler C, Brinker A, Bourenkov G, Pegoraro S, Moroder L, Bartunik H, Hartl FU, Moarefi I (2000) Structure of TPR domain-peptide complexes: critical elements in the assembly of the Hsp70-Hsp90 multichaperone machine. *Cell* 101: 199–210
- Shirane M, Nakayama KI (2003) Inherent calcineurin inhibitor FKBP38 targets Bcl-2 to mitochondria and inhibits apoptosis. *Nat Cell Biol* 5: 28–37
- Silverstein AM, Galigniana MD, Kanelakis KC, Radanyi C, Renoir JM, Pratt WB (1999) Different regions of the immunophilin FKBP52 determine its association with the glucocorticoid receptor, hsp90, and cytoplasmic dynein. *J Biol Chem* 274: 36980–36986
- Tellinghuisen TL, Marcotrigiano J, Gorbalenya AE, Rice CM (2004) The NS5A protein of hepatitis C virus is a zinc metalloprotein. *J Biol Chem* 279: 48576–48587
- Tellinghuisen TL, Marcotrigiano J, Rice CM (2005) Structure of the zinc-binding domain of an essential component of the hepatitis C virus replicase. *Nature* 435: 374–379
- Tu H, Gao L, Shi ST, Taylor DR, Yang T, Mircheff AK, Wen Y, Gorbalenya AE, Hwang SB, Lai MM (1999) Hepatitis C virus RNA polymerase and NS5A complex with a SNARE-like protein. *Virology* 263: 30–41
- Wakita T, Pietschmann T, Kato T, Date T, Miyamoto M, Zhao Z, Murthy K, Habermann A, Krausslich HG, Mizokami M, Bartenschlager R, Liang TJ (2005) Production of infectious hepatitis C virus in tissue culture from a cloned viral genome. *Nat Med* 11: 791–796
- Wang C, Gale Jr M, Keller BC, Huang H, Brown MS, Goldstein JL, Ye J (2005) Identification of FBL2 as a geranylgeranylated cellular protein required for hepatitis C virus RNA replication. *Mol Cell* 18: 425–434
- Wasley A, Alter MJ (2000) Epidemiology of hepatitis C: geographic differences and temporal trends. *Semin Liver Dis* 20: 1–16
- Watashi K, Hijikata M, Hosaka M, Yamaji M, Shimotohno K (2003) Cyclosporin A suppresses replication of hepatitis C virus genome in cultured hepatocytes. *Hepatology* 38: 1282–1288
- Watashi K, Ishii N, Hijikata M, Inoue D, Murata T, Miyanari Y, Shimotohno K (2005) Cyclophilin B is a functional regulator of hepatitis C virus RNA polymerase. *Mol Cell* 19: 111–122
- Waxman L, Whitney M, Pollak BA, Kuo LC, Darke PL (2001) Host cell factor requirement for hepatitis C virus enzyme maturation. *Proc Natl Acad Sci USA* 98: 13931–13935
- Wu B, Li P, Liu Y, Lou Z, Ding Y, Shu C, Ye S, Bartlam M, Shen B, Rao Z (2004) 3D structure of human FK506-binding protein 52: implications for the assembly of the glucocorticoid receptor/Hsp90/immunophilin heterocomplex. *Proc Natl Acad Sci USA* 101: 8348–8353
- Ye J, Wang C, Sumpter Jr R, Brown MS, Goldstein JL, Gale Jr M (2003) Disruption of hepatitis C virus RNA replication through inhibition of host protein geranylgeranylation. *Proc Natl Acad Sci USA* 100: 15865–15870
- Yi M, Lemon SM (2004) Adaptive mutations producing efficient replication of genotype 1a hepatitis C virus RNA in normal Huh7 cells. *J Virol* 78: 7904–7915
- Zhong J, Gastaminza P, Cheng G, Kapadia S, Kato T, Burton DR, Wieland SF, Uprichard SL, Wakita T, Chisari FV (2005) Robust hepatitis C virus infection *in vitro*. *Proc Natl Acad Sci USA* 102: 9294–9299



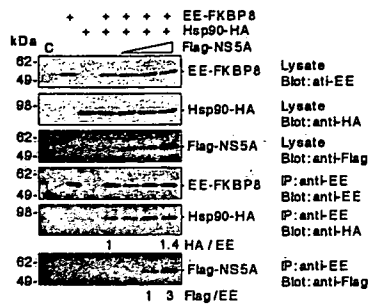
**Supplementary Figure 1. NS5A directly binds to FKBP8**

Purified thioredoxin, Trx-NS5A (A) and His-FKBP8 (B) in gel were stained with Coomassie brilliant blue G-250. These proteins were mixed and subjected to immunoprecipitation with anti-FKBP8 antibody. Precipitates were immunoblotted with anti-thioredoxin antibody (C) and stained with Coomassie brilliant blue G-250 (D).

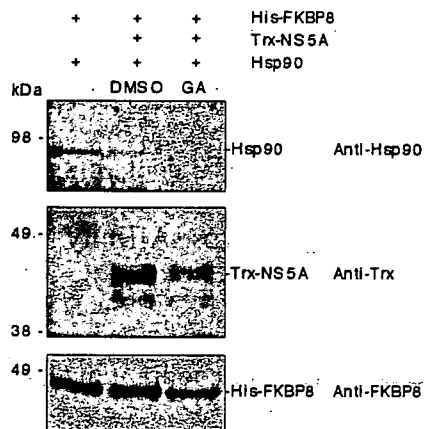


**Supplementary Figure 2. Lack of apoptosis in FKBP8-knockdown cells**

Huh7 9-13 cells were transfected with siRNA for the non-target control or FKBP8-Target 1 at a concentration of 80 nM, which was able to suppress the expression of FKBP8 (Fig. 5). Some cells were treated with 0.5 µg/ml staurosporin as a control for apoptosis. The cells were stained using the Vybrant apoptosis assay kit 1 (Molecular Probes, Eugene, OR).



**Supplementary Figure 3. Interaction of NS5A, FKBP8 and Hsp90**  
 EE-FKBP8 was co-expressed with Hsp90-HA and Flag-NS5A in 293T cells and immunoprecipitated with anti-EE antibody. Precipitates were analyzed by Western blotting by anti-EE, -HA or -Flag antibody. Effect of increase of Flag-NS5A expression on the association of FKBP8 with Hsp90 was examined by transfection with 0.1, 0.2- or 0.4  $\mu$ g of Flag-NS5A expression plasmid.



**Supplementary Figure 4. Disruption of NS5A/FKBP8/Hsp90 complexes by geldanamycin**

Purified His-FKBP8, Hsp90 and/or Trx-NS5A were mixed with DMSO or geldanamycin (GA) (100 nM) and subjected to immunoprecipitation with anti-FKBP8 antibody. Precipitates were immunoblotted with antibody to Hsp90, thioredoxin, or FKBP8.

## Supplementary materials and methods

### Preparation of monoclonal antibody to FKBP8

Glutathione-S-transferase-fused human FKBP8 (GST-FKBP8) was expressed in *Escherichia coli* strain JM109 transformed with pGEX-4T3 containing FKBP8 gene. GST-FKBP8 was purified with Glutathione-conjugated Sepharose Affinity Matrix (Amersham Pharmacia Biotech, Franklin Lakes, NJ). Purified GST- FKBP8 was immunized to *Balb/c* mouse. Lymphonodus cells were obtained after 5 boost immunizations and were fused to mouse myeloma PAI cells. The resulting hybridomas were screened by enzyme-linked immuno-sorbent assay using GST and GST-FKBP8. The selected clones were further screened by flow cytometry using 293T cells expressing HA-FKBP8 (O'Reilly *et al.*, 1998). Among several positive clones, two clones strongly reactive to human FKBP8 were designated as KDM-11 and 19 (IgG2b). Antibodies were purified from supernatants of cell culture by Protein G Sepharose 4B beads (Amersham).

### Preparation of recombinant proteins

His<sub>6</sub>-tagged FKBP8 (His-FKBP8) and thioredoxin-fused NS5A (aa 25-213, domain I) (Trx-NS5A) were generated from recombinant *Escherichia coli*. Either pET30a encoding FKBP8 or pET32a encoding NS5A (aa 25-213) was introduced into *E. coli* strain BL21(DE3). Ten milliliter of overnight culture was added into 1 L of 2 x YT medium and was incubated at 37°C. When the absorbance of culture supernatant indicated 0.4 OD<sub>600</sub>, isopropyl beta-thiogalactoside (IPTG) was added at final concentration of 0.4 mM and was then incubated at 20°C overnight. After centrifugation, the cell pellet was washed once with 10 ml phosphate buffered saline (PBS). The washed cell pellet was suspended in 40 ml lysis buffer (50mM phosphate buffer [pH 8.0] containing 150mM NaCl, 1% Triton X-100 and 0.2 µg/ml lysozyme) and was incubated at 4°C for 2h. After freezing and thawing, the mixture was sonicated at 4°C for 5 min and was treated with 0.02 mg/ml of DNase at room temperature for 5 min. The cell lysates were centrifuged at 10,000 x g for 5 min. The resulting supernatant



was mixed with 0.5 ml of Nickel agarose beads (Sigma, St. Louis, MO) and was rotated at 4°C for 60 min. The Nickel beads were washed twice with PBS containing 10 mM imidazole. The recombinant protein was eluted from Nickel beads with PBS containing 0.25 M imidazole. Bovine Hsp90 was purchased from Sigma. Bovine Hsp90- $\alpha$  shares 99.5% amino acid identity to human Hsp90- $\alpha$ .

### Reference

- O'Reilly, L.A., Cullen, L., Moriishi, K., O'Connor, L., Huang, D.C. and Strasser, A. (1998) Rapid hybridoma screening method for the identification of monoclonal antibodies to low-abundance cytoplasmic proteins. *Biotechniques*, **25**, 824-830.

## Differential roles of MDA5 and RIG-I helicases in the recognition of RNA viruses

Hiroki Kato<sup>1,3\*</sup>, Osamu Takeuchi<sup>1,3\*</sup>, Shintaro Sato<sup>3</sup>, Mitsutoshi Yoneyama<sup>4</sup>, Masahiro Yamamoto<sup>1</sup>, Kosuke Matsui<sup>1</sup>, Satoshi Uematsu<sup>1</sup>, Andreas Jung<sup>1</sup>, Taro Kawai<sup>3</sup>, Ken J. Ishii<sup>3</sup>, Osamu Yamaguchi<sup>5</sup>, Kinya Otsu<sup>5</sup>, Tohru Tsujimura<sup>6</sup>, Chang-Sung Koh<sup>7</sup>, Caetano Reis e Sousa<sup>8</sup>, Yoshiharu Matsuura<sup>2</sup>, Takashi Fujita<sup>4</sup> & Shizuo Akira<sup>1,3</sup>

The innate immune system senses viral infection by recognizing a variety of viral components (including double-stranded (ds)RNA) and triggers antiviral responses<sup>1,2</sup>. The cytoplasmic helicase proteins RIG-I (retinoic-acid-inducible protein 1; also known as Ddx58) and MDA5 (melanoma-differentiation-associated gene 5, also known as Ifih1 or Helicard) have been implicated in viral dsRNA recognition<sup>3-7</sup>. *In vitro* studies suggest that both RIG-I and MDA5 detect RNA viruses and polyinosine-polycytidylic acid (poly(I:C)), a synthetic dsRNA analogue<sup>3</sup>. Although a critical role for RIG-I in the recognition of several RNA viruses has been clarified<sup>8</sup>, the functional role of MDA5 and the relationship between these dsRNA detectors *in vivo* are yet to be determined. Here we use mice deficient in MDA5 (*MDA5*<sup>-/-</sup>) to show that MDA5 and RIG-I recognize different types of dsRNAs: MDA5 recognizes poly(I:C), and RIG-I detects *in vitro* transcribed dsRNAs. RNA viruses are also differentially recognized by RIG-I and MDA5. We find that RIG-I is essential for the production of interferons in response to RNA viruses including paramyxoviruses, influenza virus and Japanese encephalitis virus, whereas MDA5 is critical for picornavirus detection. Furthermore, *RIG-I*<sup>-/-</sup> and *MDA5*<sup>-/-</sup> mice are highly susceptible to infection with these respective RNA viruses compared to control mice. Together, our data show that RIG-I and MDA5 distinguish different RNA viruses and are critical for host antiviral responses.

Host pattern recognition receptors, such as Toll-like receptors (TLRs) and helicase family members, have an essential role in the recognition of molecular patterns specific for different viruses, including DNA, single-stranded (ss)RNA, dsRNA and glycoproteins<sup>9,10</sup>. dsRNA can be generated during viral infection as a replication intermediate for RNA viruses. TLR3, which localizes in the endosomal membrane, has been shown to recognize viral dsRNA as well as the synthetic dsRNA analogue poly(I:C) (refs 11; 12). The cytoplasmic proteins RIG-I and MDA5 have also been identified as dsRNA detectors<sup>3-5,7,13</sup>. RIG-I and MDA5 contain two caspase-recruitment domains (CARDs) and a DExD/H-box helicase domain. RIG-I recruits a CARD-containing adaptor, IPS-1 (also known as MAVS, VISA or Cardif)<sup>14-17</sup>. IPS-1 relays the signal to the kinases TBK1 and IKK- $\epsilon$ , which phosphorylate interferon-regulatory factor-3 (IRF-3) and IRF-7, transcription factors essential for the expression of type-I

interferons<sup>18-22</sup>. In contrast, TLR3 activates TBK1 and IKK- $\epsilon$  through the TIR-domain-containing adaptor TRIF (also known as Ticam1)<sup>12</sup>.

*In vitro* studies have shown that both RIG-I and MDA5 can bind to poly(I:C) and respond to poly(I:C) and RNA viruses<sup>6</sup>. We have generated *RIG-I*<sup>-/-</sup> mice, and show that RIG-I is essential eliciting the immune responses against several RNA viruses, including Newcastle disease virus (NDV), Sendai virus (SeV) and vesicular stomatitis virus (VSV), in various cells except for plasmacytoid dendritic cells (pDCs)<sup>8</sup>. Hepatitis C virus and Japanese encephalitis virus are also reported to be recognized by RIG-I *in vitro*<sup>23,24</sup>.

The *in vivo* functional relationship between RIG-I and MDA5 remains to be determined. To investigate a functional role for MDA5 *in vivo*, we generated *MDA5*<sup>-/-</sup> mice and investigated viral recognition (Supplementary Fig. 1). In contrast to *RIG-I*<sup>-/-</sup> mice, which are mostly embryonic lethal, *MDA5*<sup>-/-</sup> mice are born in a mendelian ratio, grow healthily and do not show gross developmental abnormalities until 24 weeks of age. Flow cytometric analysis of leukocytes from the spleen and lymph nodes (staining for CD3, B220 and CD11c) revealed that the composition of lymphocytes and dendritic cells is similar in wild-type and *MDA5*<sup>-/-</sup> mice (data not shown).

TLR3, RIG-I and MDA5 have been implicated in the recognition of poly(I:C) and the subsequent induction of antiviral responses. However, their exact contribution to *in vivo* responses against dsRNA has yet to be clarified. We therefore examined the *in vivo* responses to poly(I:C) in mice lacking RIG-I, MDA5 or TRIF, or both MDA5 and TRIF. Administration of poly(I:C) led to rapid induction of the cytokines interferon- $\alpha$  (IFN- $\alpha$ ), IFN- $\beta$ , interleukin-6 (IL-6) and IL-12 in sera of both wild-type and *RIG-I*<sup>-/-</sup> mice (Fig. 1a and Supplementary Fig. 2a). In contrast, *MDA5*<sup>-/-</sup> mice failed to produce IFN- $\alpha$  and IFN- $\beta$  in response to poly(I:C), and production of IL-6 and IL-12p40 was also significantly impaired (Fig. 1b). Although *Trif*<sup>-/-</sup> mice produced normal amounts of IFN- $\alpha$ , they also showed severely impaired production of IL-12p40 and partial impairment in IL-6 production. *MDA5*<sup>-/-</sup>; *Trif*<sup>-/-</sup> double-knock-out mice failed to induce IFN- $\alpha$ , IL-6 and IL-12p40 in response to poly(I:C). These results indicate that MDA5 is essential for poly(I:C)-induced IFN- $\alpha$  production and TLR3 signalling is critical for IL-12 production, whereas both MDA5 and TLR3 regulate IL-6 production.

<sup>1</sup>Department of Host Defense, <sup>2</sup>Department of Molecular Virology, Research Institute for Microbial Diseases, Osaka University, and <sup>3</sup>ERATO, Japan Science and Technology Agency, 3-1 Yamada-oka, Suita, Osaka 565-0871, Japan. <sup>4</sup>Department of Genetics and Molecular Biology, Institute for Virus Research, Kyoto University, 53 Kawahara-cho, Shogoin, Sakyo-ku, Kyoto 606-8507, Japan. <sup>5</sup>Department of Cardiovascular Medicine, Osaka University Graduate School of Medicine, 2-2 Yamada-oka, Suita, Osaka 565-0871, Japan. <sup>6</sup>Department of Pathology, Hyogo College of Medicine, 1-1 Mukogawa-cho, Nishinomiya, Hyogo 663-8501, Japan. <sup>7</sup>Department of Medical Technology, Shinshu University School of Allied Medical Sciences, 3-1-1 Asahi, Matsumoto 390-8621, Japan. <sup>8</sup>Immunobiology Laboratory, Cancer Research UK London Research Institute, Lincoln's Inn Fields Laboratories, 44 Lincoln's Inn Fields, London WC2A 3PX, UK.

\*These authors contributed equally to this work.

When bone-marrow-derived dendritic cells generated by granulocyte-macrophage colony-stimulating factor (GM-CSF) were incubated in the presence of poly(I:C), production of IFN- $\alpha$  and IFN- $\beta$  was severely impaired in  $MDA5^{-/-}$ , but not in  $RIG-I^{-/-}$  or  $Trif^{-/-}$ , GM-CSF-DCs (Fig. 1c and Supplementary Fig. 2b). Even when poly(I:C) was transfected into GM-CSF-DCs using lipofectamine, poly(I:C) induced IFN- $\beta$  production in an MDA5-dependent, but not a RIG-I- or TRIF-dependent, manner (Fig. 1d). IFN- $\beta$  production in response to poly(I:C) was also impaired in  $MDA5^{-/-}$  mouse embryonic fibroblasts (MEFs) (Fig. 1e), indicating that poly(I:C) is primarily recognized by MDA5, not RIG-I and TLR3, in these cells.

dsRNAs transcribed *in vitro* (Supplementary Fig. 2c) also stimulated MEFs to produce IFN- $\beta$ . Unlike for poly(I:C), wild-type and  $MDA5^{-/-}$  MEFs produced comparable amounts of IFN- $\beta$  (Fig. 1e) in response to *in vitro* transcribed dsRNAs. In contrast,  $RIG-I^{-/-}$  MEFs did not produce detectable amounts of IFN- $\beta$ , indicating that RIG-I is essential for the detection of *in vitro* transcribed dsRNAs. As RIG-I, but not MDA5, is responsible for IFN- $\beta$  production in response to dsRNAs of various lengths, these helicases probably distinguish nucleotide structure or sequence, but not length. Together, these results indicate that MDA5 and RIG-I are involved

in the detection of poly(I:C) and *in vitro* transcribed dsRNAs, respectively.

This finding led us to hypothesize that RIG-I and MDA5 are involved in the detection of different RNA viruses. We have previously shown that a set of negative-sense RNA viruses are recognized by RIG-I<sup>8</sup>. We first examined IFN- $\beta$  and IFN- $\alpha$  production in  $MDA5^{-/-}$  MEFs in response to a set of negative-sense ssRNA viruses, including NDV, SeV, VSV and influenza virus. As infection with most of the wild-type viruses (except NDV) failed to induce type-I interferons in MEFs, owing to suppression of interferon responses by viral proteins (data not shown), we also used mutant viruses lacking viral interferon-inhibitory proteins. As shown in Fig. 2a and Supplementary Fig. 4b, wild-type MEFs produce IFN- $\beta$  and IFN- $\alpha$  in response to these mutant viruses. Production of type-I interferons was severely impaired in  $RIG-I^{-/-}$  MEFs compared to wild-type cells, but MDA5 was dispensable for the production of type-I interferons. Japanese encephalitis virus (JEV), a positive-sense ssRNA virus belonging to the flavivirus family, also required RIG-I, but not MDA5, for IFN- $\beta$  production (Fig. 2b).

We then examined the interferon responses of MEFs to encephalomyocarditis virus (EMCV), a positive-sense ssRNA virus belonging to the picornavirus family. EMCV-induced IFN- $\beta$  production was abrogated in  $MDA5^{-/-}$  MEFs (Fig. 2c). In contrast, wild-type and  $RIG-I^{-/-}$  MEFs produced comparable amounts of IFN- $\beta$ , indicating that EMCV is specifically recognized by MDA5. The induction of genes encoding IFN- $\beta$ , IP-10 and IL-6 in response to EMCV was abrogated in  $MDA5^{-/-}$  macrophages (Supplementary Fig. 3d). The synthesis of cellular proteins in  $MDA5^{-/-}$  MEFs was progressively inhibited during EMCV infection, to an extent and with kinetics similar to wild-type MEFs (Supplementary Fig. 5), indicating that the EMCV infection was established in wild-type and  $MDA5^{-/-}$  MEFs in a similar manner. Moreover, other viruses belonging to the picornavirus family (Theiler's and Mengo viruses) also induced IFN- $\alpha$  through MDA5 (Supplementary Fig. 4d). Furthermore, the production of IFN- $\beta$  in response to SeV and EMCV was impaired in  $RIG-I^{-/-}$  and  $MDA5^{-/-}$  GM-CSF-DCs, respectively (Fig. 2d, e), indicating that conventional dendritic cells (cDCs) also use these helicases for the differential recognition of viruses. EMCV-induced production of IL-6 was also abrogated in  $MDA5^{-/-}$ , but not  $RIG-I^{-/-}$ , cDCs (Supplementary Fig. 4c). Therefore, MDA5 is critical for the regulation of pro-inflammatory cytokines as well as type-I interferons in response to EMCV.

We next examined whether viral RNAs derived from VSV and EMCV recapitulate the production of interferons through MDA5 and RIG-I. When transfected into GM-CSF-DCs by lipofection, RNAs prepared from VSV or EMCV induced production of IFN- $\alpha$  in a RIG-I- or MDA5-dependent manner, respectively (Fig. 2f). We also performed reconstitution experiments by transfecting RIG-I or MDA5 expression vectors into  $RIG-I^{-/-}$ ;  $MDA5^{-/-}$  MEFs, in which IFN- $\beta$  induction was completely abrogated in response to infection with EMCV or SeV Cm (SeV with a mutated C protein) (Fig. 2g). The ectopic expression of human RIG-I, but not MDA5, activated the *Ifnb* promoter in response to SeV Cm. Reciprocally, cells expressing human MDA5, but not RIG-I, activated the *Ifnb* promoter in response to EMCV in a dose-dependent manner (Fig. 2h). These results indicate that human RIG-I and MDA5 recognize different RNA viruses by recognizing viral RNAs.

Previous studies have shown that pDCs use mainly the TLR system instead of RIG-I in the recognition of several RNA viruses<sup>8</sup>. MyD88 is an adaptor protein essential for TLR signalling (except through TLR3). We purified B220<sup>+</sup> pDCs from Flt3L-generated bone-marrow-derived dendritic cells (Flt3L-DCs) and infected them with EMCV. pDCs from *Myd88*<sup>-/-</sup>, but not *MDA5*<sup>-/-</sup>, mice showed a profound defect in IFN- $\alpha$  production (Supplementary Fig. 6). Reciprocally, MDA5, but not MyD88, is required for the production of IFN- $\alpha$  in B220<sup>-</sup> cDCs purified from Flt3L-DCs (Supplementary Fig. 6). These results indicate that both MDA5 and RIG-I are

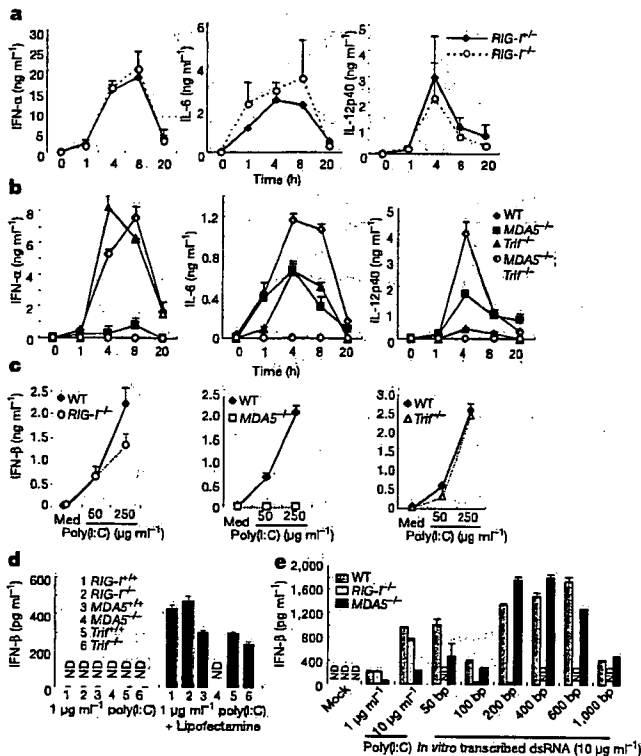


**Figure 1** Roles of MDA5, RIG-I and TRIF in the recognition of synthesized dsRNAs and dsRNA analogues. **a**, **b**,  $RIG-I^{-/-}$  and littermate  $RIG-I^{+/+}$  mice (**a**) or wild-type (WT),  $MDA5^{-/-}$ ,  $Trif^{-/-}$  or  $MDA5^{-/-}$ ;  $Trif^{-/-}$  double-knockout mice (**b**) were injected intravenously with 200  $\mu$ g poly(I:C) for the indicated periods, and IFN- $\alpha$ , IL-6 and IL-12p40 production was measured in serum by ELISA. Data show mean  $\pm$  s.d. **c**, GM-CSF-DCs from  $RIG-I^{-/-}$ ,  $MDA5^{-/-}$ ,  $TRIF^{-/-}$  and littermate control mice were incubated in the presence of 50 or 250  $\mu$ g ml<sup>-1</sup> poly(I:C) for 24 h. IFN- $\beta$  production in the cell culture supernatants was measured by ELISA. Med, medium only. **d**, GM-CSF-DCs were treated with 1  $\mu$ g ml<sup>-1</sup> poly(I:C) complexed with or without lipofectamine 2000 for 24 h, and IFN- $\beta$  production was measured. **e**, Wild-type,  $RIG-I^{-/-}$  and  $MDA5^{-/-}$  MEFs were treated with poly(I:C) or *in vitro* transcribed dsRNAs of indicated lengths complexed with lipofectamine 2000 for 12 h, and IFN- $\beta$  production was measured. Error bars indicate s.d. of triplicate wells in a single experiment; data are representative of three independent experiments. ND, not detected.

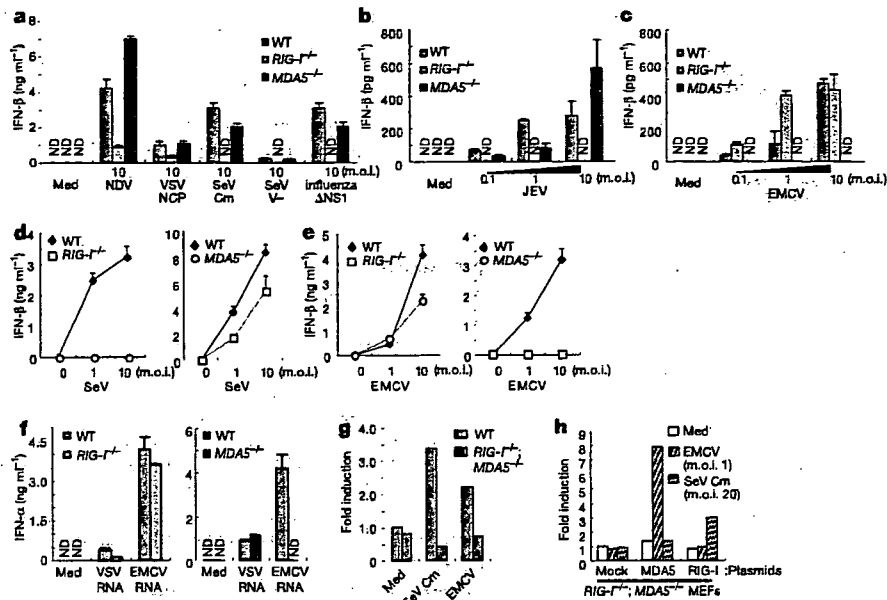


**Figure 2 | Differential viral recognition by RIG-I and MDA5.** **a**, Wild-type, *RIG-I*<sup>-/-</sup> and *MDA5*<sup>-/-</sup> MEFs were exposed to negative-sense ssRNA viruses, including NDV, VSV lacking a variant of M protein (NCP), SeV with a mutated C protein (Cm), SeV lacking V protein (V<sup>-</sup>), and influenza virus lacking the NS1 protein ( $\Delta$ NS1) for 24 h. IFN- $\beta$  production in the culture supernatants was measured by ELISA. **b, c**, Wild-type, *RIG-I*<sup>-/-</sup> and *MDA5*<sup>-/-</sup> MEFs were exposed to the positive-sense ssRNA viruses JEV (**b**) and EMCV (**c**), and IFN- $\beta$  production was measured. **d, e**, GMCSF-DCs from *RIG-I*<sup>-/-</sup> and *MDA5*<sup>-/-</sup> mice and their littermate wild-type mice were infected with an increasing m.o.i. of SeV V<sup>-</sup> (**d**) or EMCV (**e**) for 24 h, and IFN- $\beta$  production was measured. **f**, Wild-type, *RIG-I*<sup>-/-</sup> and *MDA5*<sup>-/-</sup>

GMCSF-DCs were treated with RNAs directly prepared from VSV and EMCV (complexed with lipofectamine 2000) for 24 h, and IFN- $\alpha$  production was measured. **g**, Wild-type and *RIG-I*<sup>-/-</sup>; *MDA5*<sup>-/-</sup> MEFs were transiently transfected with a reporter construct containing the *Irfn* promoter and exposed to SeV Cm or EMCV for 24 h. Cell lysates were then prepared and subjected to a luciferase assay. **h**, *RIG-I*<sup>-/-</sup>; *MDA5*<sup>-/-</sup> MEFs were transiently transfected with the *Irfn* promoter construct together with expression plasmids encoding human RIG-I or MDA5. The cells were then infected with EMCV or SeV Cm for 24 h and were subjected to a luciferase assay. Error bars in **a-g** indicate s.d. of triplicate wells in a single experiment; data are representative of three independent experiments. ND, not detected.

dispensable for the viral induction of IFN- $\alpha$  in pDCs.

We next examined the *in vivo* roles of MDA5 and RIG-I in host defence against viral infection. Although most *RIG-I*<sup>-/-</sup> mice are embryonic lethal<sup>8</sup>, we could efficiently obtain live adult mice by intercrossing the *RIG-I*<sup>+/-</sup> mice obtained after *RIG-I*<sup>+/-</sup>  $\times$  ICR crosses (Supplementary Table 1). When the mice were infected with JEV, serum IFN- $\alpha$  levels were markedly decreased in *RIG-I*<sup>-/-</sup> mice compared to littermate *RIG-I*<sup>+/-</sup> mice. In contrast, *MDA5*<sup>-/-</sup> mice did not show a defect in JEV-induced systemic IFN- $\alpha$  production (Fig. 3a). IFN- $\alpha$  production was partially impaired in *Myd88*<sup>-/-</sup> mice compared to wild-type mice, but the extent of this impairment was far less than in *RIG-I*<sup>-/-</sup> mice (Fig. 3a). These data suggest that the TLR system is not critical for the induction of serum IFN- $\alpha$  *in vivo* in response to JEV. Consistent with this finding, *RIG-I*<sup>-/-</sup> mice, but not *MDA5*<sup>-/-</sup> or *Myd88*<sup>-/-</sup> mice, were more susceptible to JEV infection than control mice (Fig. 3b). Furthermore, *RIG-I*<sup>-/-</sup> mice, but not *MDA5*<sup>-/-</sup> mice, succumbed to VSV infection, consistent with abrogated interferon responses (Supplementary Fig. 7). Thus, RIG-I-mediated recognition of a specific set of viruses has a critical role in antiviral host defence *in vivo*.

We next challenged the mice with EMCV as a model virus that is recognized by MDA5. Induction of IFN- $\beta$ , IFN- $\alpha$ , RANTES and IL-6 was severely impaired in the sera of *MDA5*<sup>-/-</sup> mice (Fig. 4a and Supplementary Fig. 8). *MDA5*<sup>-/-</sup> mice and mice null for the IFN- $\alpha/\beta$  receptor (*Irfn1*<sup>-/-</sup>) were highly susceptible to EMCV infection (viral titre of  $1 \times 10^2$  plaque-forming units (p.f.u.)) compared to littermate controls ( $P < 0.01$ ) (Fig. 4b). In contrast, deficiency of neither RIG-I nor TLR3 affected the survival of mice infected with EMCV. Consistent with a previous report<sup>22</sup>, *Myd88*<sup>-/-</sup> mice were modestly susceptible to EMCV infection compared to wild-type mice, implying that pDC-mediated responses are not critical for eliminating EMCV (Fig. 4b).

It is known that EMCV preferentially infects cardiomyocytes and causes myocarditis. Consistent with increased susceptibility to EMCV, viral titre in the heart was much higher in *MDA5*<sup>-/-</sup> mice compared to control mice (Fig. 4c). Histological analysis of hearts two days after EMCV infection revealed that focal necrosis of

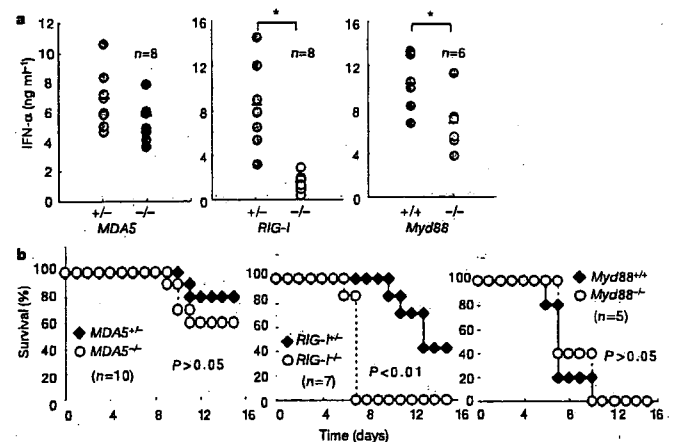


**Figure 3 | Susceptibility of *RIG-I*<sup>-/-</sup> and *MDA5*<sup>-/-</sup> mice to JEV infection.** **a**, *RIG-I*<sup>+/-</sup>, *RIG-I*<sup>-/-</sup>, *MDA5*<sup>+/-</sup> and *MDA5*<sup>-/-</sup> mice ( $n = 8$ ), and *Myd88*<sup>+/+</sup> or *Myd88*<sup>-/-</sup> mice ( $n = 6$ ), were injected intravenously with  $2 \times 10^7$  p.f.u. JEV. Sera were collected 24 h after injection, and IFN- $\alpha$  production levels measured by ELISA. Circles represent individual mice, bars indicate mean values. Asterisk,  $P < 0.05$  versus controls (*t*-test). **b**, The survival of 6-week-old mice (genotypes as indicated) infected intravenously with  $2 \times 10^7$  p.f.u. JEV. Mice were monitored for 15 days ( $P < 0.01$  between *RIG-I*<sup>-/-</sup> mice and their littermate controls, generalized Wilcoxon test).

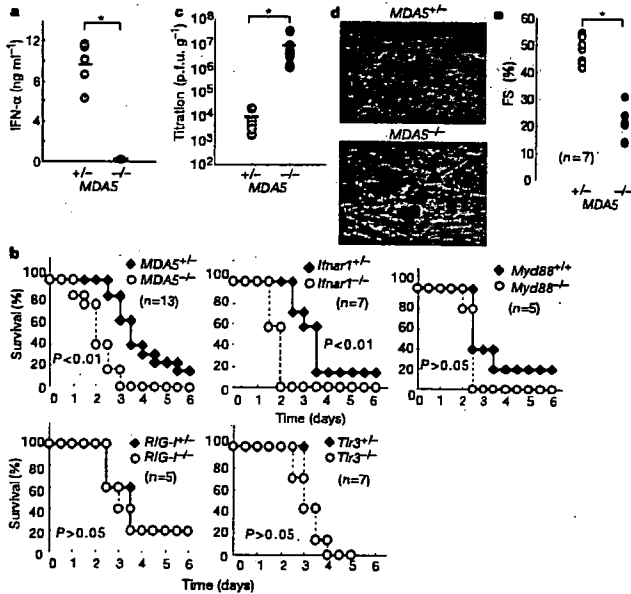


**Figure 4 | Role of MDA5 in host defence against EMCV infection.**

**a**, MDA5<sup>+/+</sup> and MDA5<sup>-/-</sup> mice ( $n = 5$ ) were inoculated intravenously with  $1 \times 10^7$  p.f.u. EMCV. Sera were prepared 4 h after injection and IFN- $\alpha$  production levels determined by ELISA. **b**, The survival of 6-week-old mice (genotypes as indicated) infected with  $1 \times 10^2$  p.f.u. EMCV intraperitoneally was monitored every 12 h for six days ( $P < 0.01$  between MDA5<sup>-/-</sup> or *Ifnar1*<sup>-/-</sup> mice and their littermate controls, generalized Wilcoxon test). **c**, MDA5<sup>+/+</sup> and MDA5<sup>-/-</sup> mice were infected intraperitoneally with  $1 \times 10^2$  p.f.u. EMCV. After 48 h, mice were killed and virus titres in hearts were determined by plaque assay. **d**, Heart sections of MDA5<sup>+/+</sup> and MDA5<sup>-/-</sup> mice, two days after infection, were assessed for histological changes using haematoxylin and eosin staining. Arrow indicates the focal necrosis of cardiomyocytes. **e**, Cardiac function of mice 48 h after EMCV infection was assessed by echocardiography (see Supplementary Fig. 8b). The fractional shortening (FS) after infection determined by transthoracic M-mode echocardiographic tracings is shown. Asterisk,  $P < 0.05$  versus MDA5<sup>+/+</sup> mice ( $t$ -test).

cardiomyocytes had developed in MDA5<sup>-/-</sup> mice, but wild-type hearts showed no histological abnormalities at this time point (Fig. 4d). Notably, no infiltration of immune cells was observed in either wild-type or MDA5<sup>-/-</sup> heart sections at this time point. However, when cardiac performance was analysed by echocardiography two days after infection (Fig. 4e), cardiac contractility was severely depressed in MDA5<sup>-/-</sup> mice (fractional shortening  $48.2 \pm 4.9\%$  in MDA5<sup>+/+</sup> mice,  $21.2 \pm 5.8\%$  in MDA5<sup>-/-</sup> mice), indicating that MDA5<sup>-/-</sup> mice developed severe heart failure due to virus-induced cardiomyopathy. Thus, MDA5-mediated recognition of EMCV is a prerequisite for triggering antiviral responses as well as for prevention of myocardial dysfunction.

Together, our results demonstrate that RIG-I and MDA5 have essential roles in the recognition of different groups of RNA viruses, as well as in the subsequent production of type-I interferons and pro-inflammatory cytokines. We have found that poly(I:C) and *in vitro* transcribed dsRNA are recognized by MDA5 and RIG-I, respectively; this is in contrast to results from previous *in vitro* studies. RIG-I probably recognizes dsRNA generated over the course of RNA virus replication, as all *in vitro* transcribed dsRNAs tested except for poly(I:C) induced type-I interferons through RIG-I. In contrast, the endogenous ligand of MDA5 remains enigmatic. Moreover, how RIG-I and MDA5 differentially recognize natural dsRNAs is undetermined. Given that the helicase domains of RIG-I and MDA5 bind to dsRNA, analyses of the crystal structures of these domains should help achieve a better understanding of the molecular mechanisms underlying this differential recognition.

Furthermore, it is still possible that unknown dsRNA-binding proteins also function as direct receptors for viral RNAs.

Finally, the picornavirus family contains several viruses that are pathogenic for humans, including poliovirus, rhinovirus and the virus causing foot-and-mouth-disease. Our studies suggest that human MDA5 and RIG-I also recognize RNA viruses. Thus, identification of therapeutic agents that modify RIG-I or MDA5 may lead to antiviral strategies against selected viruses.

## METHODS

**Mice, cells and reagents.** The generation of MDA5<sup>-/-</sup> mice is described in the Supplementary Information. *Myd88*<sup>-/-</sup>, *Tlr3*<sup>-/-</sup> and *Trif*<sup>-/-</sup> mice have been described previously<sup>23</sup>. *Ifnar1*<sup>-/-</sup> mice have also been described previously<sup>23</sup>. RIG-I<sup>-/-</sup> mice in a 129Sv  $\times$  C57BL/6 background were crossed with ICR mice, and the resulting RIG-I<sup>-/-</sup> mice were further intercrossed. Interbreeding of these RIG-I<sup>-/-</sup> mice produced healthy and fertile RIG-I<sup>-/-</sup> offspring, although their number was less than half that of RIG-I<sup>+/+</sup> progeny (Supplementary Table 1). RIG-I<sup>-/-</sup> and RIG-I<sup>+/+</sup> littermate mice were used for *in vivo* experiments. RIG-I<sup>-/-</sup>; MDA5<sup>-/-</sup> mice in a 129Sv  $\times$  C57BL/6 background were lethal at embryonic day 12.5. Additional details regarding cells, reagents and the preparation of *in vitro* transcribed dsRNA are provided in the Supplementary Information.

**Viruses.** NDV (ref. 3), VSV, VSV lacking a variant of M protein (NCP) (ref. 8), influenza virus lacking the NS1 protein ( $\Delta$ NS1) (ref. 26), JEV (ref. 27) and EMCV (ref. 3) have been described previously. SeV and SeV lacking the V protein (V<sup>-</sup>) or with mutated C proteins (Cm) were provided by A. Kato<sup>28</sup>.

**Luciferase assay.** Wild-type or RIG-I<sup>-/-</sup>; MDA5<sup>-/-</sup> MEFs were transiently transfected with a reporter construct containing the *Ifnb* promoter together with an empty vector (mock), or RIG-I or MDA5 expression vectors. As an internal control, a *Renilla* luciferase construct was transfected. Transfected cells were untreated or infected with EMCV or SeV-Cm (m.o.i. 20) for 24 h. The cells were lysed and subjected to a luciferase assay using a dual-luciferase reporter assay system (Promega) according to the manufacturer's instructions.

**Analysis of mice after EMCV infection.** Methods for plaque assays, histological analysis and echocardiography are described in the Supplementary Information.

**Measurement of cytokine production.** Cell culture supernatants were collected and analysed for IFN- $\beta$ , IFN- $\alpha$ , IL-6 or IL-12p40 production using enzyme-linked immunosorbent assays (ELISAs). ELISA kits for mouse IFN- $\alpha$  and IFN- $\beta$  were purchased from PBL Biomedical Laboratories, and those for IL-6, IL-12p40 and RANTES were obtained from R&D Systems.

**Statistical analysis.** Kaplan-Meier plots were constructed and a generalized Wilcoxon test was used to test for differences in survival between control and mutant mice after viral infection. Statistical significance of any differences in cytokine concentration and EMCV titres was determined using Student's  $t$ -tests.

Received 30 January; accepted 20 March 2006.

Published online 9 April 2006.

1. Akira, S., Uematsu, S. & Takeuchi, O. Pathogen recognition and innate immunity. *Cell* 124, 783–801 (2006).
2. Katze, M. G., He, Y. & Gale, M. Jr. Viruses and interferon: A fight for supremacy. *Nature Rev. Immunol.* 2, 675–687 (2002).
3. Yoneyama, M. et al. The RNA helicase RIG-I has an essential function in double-stranded RNA-induced innate antiviral responses. *Nature Immunol.* 5, 730–737 (2004).
4. Kang, D. C. et al. *mda-5*: An interferon-inducible putative RNA helicase with double-stranded RNA-dependent ATPase activity and melanoma growth-suppressive properties. *Proc. Natl Acad. Sci. USA* 99, 637–642 (2002).
5. Andrejeva, J. et al. The V proteins of paramyxoviruses bind the IFN- $\beta$  inducible RNA helicase, *mda-5*, and inhibit its activation of the IFN- $\beta$  promoter. *Proc. Natl Acad. Sci. USA* 101, 17264–17269 (2004).
6. Yoneyama, M. et al. Shared and unique functions of the DEXD/H-box helicases RIG-I, MDA5, and LGP2 in antiviral innate immunity. *J. Immunol.* 175, 2851–2858 (2005).
7. Rothenfusser, S. et al. The RNA helicase Lgp2 inhibits TLR-independent sensing of viral replication by retinoic acid-inducible gene-1. *J. Immunol.* 175, 5260–5268 (2005).
8. Kato, H. et al. Cell type-specific involvement of RIG-I in antiviral response. *Immunity* 23, 19–28 (2005).
9. Iwasaki, A. & Medzhitov, R. Toll-like receptor control of the adaptive immune responses. *Nature Immunol.* 5, 987–995 (2004).
10. Beutler, B. Inferences, questions and possibilities in Toll-like receptor signalling. *Nature* 430, 257–263 (2004).
11. Alexopoulou, L., Holt, A. C., Medzhitov, R. & Flavell, R. A. Recognition of double-stranded RNA and activation of NF- $\kappa$ B by Toll-like receptor 3. *Nature* 413, 732–738 (2001).

12. Yamamoto, M. *et al.* Role of adaptor TRIF in the MyD88-independent toll-like receptor signaling pathway. *Science* 301, 640–643 (2003).
13. Kovacsics, M. *et al.* Overexpression of Helicard, a CARD-containing helicase cleaved during apoptosis, accelerates DNA degradation. *Curr. Biol.* 12, 838–843 (2002).
14. Kawai, T. *et al.* IPS-1, an adaptor triggering RIG-I- and Mda5-mediated type I interferon induction. *Nature Immunol.* 6, 981–988 (2005).
15. Seth, R. B., Sun, L., Ea, C. K. & Chen, Z. J. Identification and characterization of MAVS, a mitochondrial antiviral signaling protein that activates NF- $\kappa$ B and IRF 3. *Cell* 122, 669–682 (2005).
16. Xu, L. G. *et al.* VISA is an adapter protein required for virus-triggered IFN- $\beta$  signaling. *Mol. Cell* 19, 727–740 (2005).
17. Meylan, E. *et al.* Cardif is an adaptor protein in the RIG-I antiviral pathway and is targeted by hepatitis C virus. *Nature* 437, 1167–1172 (2005).
18. Fitzgerald, K. A. *et al.* IKK $\epsilon$  and TBK1 are essential components of the IRF3 signaling pathway. *Nature Immunol.* 4, 491–496 (2003).
19. Sharma, S. *et al.* Triggering the interferon antiviral response through an IKK-related pathway. *Science* 300, 1148–1151 (2003).
20. Hemmi, H. *et al.* The roles of two  $\kappa$ B kinase-related kinases in lipopolysaccharide and double stranded RNA signaling and viral infection. *J. Exp. Med.* 199, 1641–1650 (2004).
21. Sato, M. *et al.* Distinct and essential roles of transcription factors IRF-3 and IRF-7 in response to viruses for IFN- $\alpha/\beta$  gene induction. *Immunity* 13, 539–548 (2000).
22. Honda, K. *et al.* IRF-7 is the master regulator of type-I interferon-dependent immune responses. *Nature* 434, 772–777 (2005).
23. Chang, T. H., Liao, C. L. & Lin, Y. L. Flavivirus induces interferon-beta gene expression through a pathway involving RIG-I-dependent IRF-3 and PI3K-dependent NF- $\kappa$ B activation. *Microbes Infect.* 8, 157–171 (2006).
24. Melchjorsen, J. *et al.* Activation of innate defense against a paramyxovirus is mediated by RIG-I and TLR7 and TLR8 in a cell-type-specific manner. *J. Virol.* 79, 12944–12951 (2005).
25. Hoshino, K., Kaisho, T., Iwabe, T., Takeuchi, O. & Akira, S. Differential involvement of IFN- $\beta$  in Toll-like receptor-stimulated dendritic cell activation. *Int. Immunol.* 14, 1225–1231 (2002).
26. Diebold, S. S., Kaisho, T., Hemmi, H., Akira, S. & Reis e Sousa, C. Innate antiviral responses by means of TLR7-mediated recognition of single-stranded RNA. *Science* 303, 1529–1531 (2004).
27. Mori, Y. *et al.* Nuclear localization of Japanese encephalitis virus core protein enhances viral replication. *J. Virol.* 79, 3448–3458 (2005).
28. Kato, A. *et al.* Characterization of the amino acid residues of sendai virus C protein that are critically involved in its interferon antagonism and RNA synthesis down-regulation. *J. Virol.* 78, 7443–7454 (2004).

**Supplementary Information** is linked to the online version of the paper at [www.nature.com/nature](http://www.nature.com/nature).

**Acknowledgements** We thank all colleagues in our laboratory, K. Takeda, T. Shioda, E. Nakayama and K. Kiyotani for helpful discussions, A. Kato, T. Abe, Y. Mori, B. S. Kim and A. Palménberg for viruses and plasmids, M. Hashimoto for secretarial assistance, and Y. Fujiwara, M. Shiokawa, N. Kitagaki and A. Shibano for technical assistance. This work was supported by grants from the Ministry of Education, Culture, Sports, Science and Technology in Japan, and from the 21st Century Center of Excellence Program of Japan.

**Author Information** Reprints and permissions information is available at [npg.nature.com/reprintsandpermissions](http://npg.nature.com/reprintsandpermissions). The authors declare no competing financial interests. Correspondence and requests for materials should be addressed to S.A. ([sakira@biken.osaka-u.ac.jp](mailto:sakira@biken.osaka-u.ac.jp)).

## Supplementary Information

### I. Supplementary Materials and Methods

### II. Supplemental Figure Legends

### III. Supplemental Figures

### I. Supplementary Materials and Methods

#### Generation of MDA5<sup>-/-</sup> mice

The MDA5 gene was isolated from genomic DNA extracted from ES cells (GSI-I) by PCR. The targeting vector was constructed by replacing a 4.3-kb fragment encoding the MDA5 ORF (including DExH box) with a neomycin-resistance gene cassette (*neo*), and a herpes simplex virus thymidine kinase (HSV-TK) driven by PGK promoter was inserted into the genomic fragment for negative selection. After the targeting vector was transfected into ES cells, G418 and gancyclovir doubly resistant colonies were selected and screened by PCR and further confirmed by Southern blotting. Homologous recombinants were micro-injected into C57BL/6 female mice, and heterozygous F1 progenies were intercrossed in order to obtain MDA5<sup>-/-</sup> mice. MDA5<sup>-/-</sup> and littermate control mice were used throughout the experiments.

#### Cells and Reagents

RIG-I<sup>-/-</sup> or MDA5<sup>-/-</sup> MEFs were prepared from embryos under 129Sv and C57BL/6 background derived at 12.5 days postcoitum. RIG-I<sup>-/-</sup>MDA5<sup>-/-</sup> MEFs were prepared from embryos (129Sv X C57BL/6 background) at 11.5 days postcoitum. Bone marrow derived DCs were generated in RPMI 1640 medium containing 10% FCS, 50 mM 2-mercaptoethanol, and 10 ng/ml GM-CSF or 10 ng/ml Flt3L. pDCs and cDCs were isolated from Flt3L-DCs by MACS using anti-B220 and CD11c microbeads from

Miltenyi Biotech as described. Poly I:C was purchased from Amersham Biosciences. For the synthesis of poly I:C, poly I (152-539 bases) and poly C (319-1305 bases) have been separately synthesized and then annealed. Therefore, the expected length of poly I:C is 319-539 bps (Amersham Biosciences). Poly I:C was complexed with cationic lipids, Lipofectamin 2000 reagents (Invitrogen), and added to MEFs. DCs were incubated with or without Lipofectamine 2000 for stimulation.

#### Northern blot

PECs were treated with or without 1000 U/ml mouse IFN- $\beta$  (Calbiochem) for 8 h, and total RNA was extracted using TRIzol reagent (Invitrogen). RNA was electrophoresed, transferred to nylon membranes and then hybridized with indicated cDNA probes. To detect the expression of MDA5 mRNA, a 308 bp fragment (777-1084) was used as a probe. The same membrane was rehybridized with a  $\beta$ -actin probe.

#### Western blot analysis and an antibody

MEF were treated with 1000 U/ml IFN- $\beta$  for 8 h. Cells were then lysed in a lysis buffer containing 1.0% Nonidet-P40, 150 mM NaCl, 20 mM Tris-Cl (pH7.5), 1 mM EDTA and protease inhibitor cocktail (Roche). Cell lysates were dissolved by SDS-PAGE and transferred onto a PVDF membrane. The membrane was blotted with the specific antibody to MDA5 protein, and visualized with an enhanced chemiluminescence system (Perkinermer). Polyclonal anti-MDA5 antibody was raised against corresponding to amino acids 1005-1019 of mouse MDA5.

#### Preparation of in vitro transcribed dsRNA

The mouse Lamin A/C cDNA sequence was amplified by PCR and cloned into the pT7 blue T vector (Novagen) and sequenced. Various lengths of dsRNAs corresponding to the sequence of mouse Lamin A/C were generated using a T7 RiboMAX<sup>TM</sup> Express RNAi



System (Promega) according to the manufacturer's instruction. In brief, DNA fragments tagged with T7 RNA polymerase promoters corresponding to parts of Lamin A/C (50, 100, 200, 400, 600, 1000 bps) were amplified by a PCR reaction using Lamin A/C cDNA as a template, and with following primers:

T7 Lamin. Forward, TAATACGACTCACTATAGGacttggtggctgcgcaggc

T7 Lamin.50 reverse, TAATACGACTCACTATAGGtgagaagagcctcaggctcctt

T7 Lamin.100 reverse, TAATACGACTCACTATAGGcaatgtgcgcttctcactgagagcag

T7 Lamin.200 reverse, TAATACGACTCACTATAGGccactcgcctcagcatctcat

T7 Lamin.400 reverse, TAATACGACTCACTATAGGctgtccacctggctcctcatg

T7 Lamin.600 reverse, TAATACGACTCACTATAGGtcctccaggtcacgcagcttt

T7 Lamin.1000 reverse, TAATACGACTCACTATAGGggacttggtgcgcagccgcacgaac

The PCR products were purified and used as templates for *in vitro* transcription with T7 RNA polymerase. The product was annealed to form dsRNA followed by treatment with DNase and RNase to digest ssRNA and DNA. The dsRNA was further purified by isopropanol precipitation and resuspended in Nuclease-free water. The generation of dsRNAs was visualized by Agarose gel electrophoresis (Supplementary Fig. 2b). To stimulate MEFs, the dsRNA was complexed with Lipofectamine 2000, then added to the cells, and incubated for 24 hours.

#### Histological analysis

Hearts were taken from EMCV infected mice, and fixed with 3.7% formaldehyde. Transverse sections through the heart (5  $\mu$ m) were cut and stained with hematoxylin and eosin.

#### Plaque assay

Forty-eight hours after EMCV infection, Hearts were prepared and homogenized in PBS. Virus titration in the virus containing PBS was determined by standard plaque assay as

described previously<sup>8</sup>. After centrifugation, supernatants were serially diluted, and added to plates containing HeLa cells. The cells were overlaid with DMEM containing 1% low melting agarose and incubated for 48 h. Then plaques were counted.

#### Echocardiography

Two days after EMCV infection, echocardiography was performed on mice anesthetized with 2.5% avertin (8 µl/g) using ultra-sonography (SONOS-5500, equipped with a 15-MHz linear transducer, Philips Medical Systems). Hearts were imaged in a two-dimensional parasternal short-axis view, and an M-mode echocardiogram of the midventricle was recorded at the level of the papillary muscles\*. Heart rate, anterior and posterior wall thickness, and end-diastolic and end-systolic internal dimensions of the LV were obtained from the M-mode image.

#### Viruses

Mengo virus<sup>1</sup> was kindly provided by A. Palmenberg. Theiler's virus<sup>2</sup> have been described previously.

#### Preparation of viral RNA

BHK cells and L cell plated on 10 X 15 cm dishes were infected with moi= 0.01 of wt VSV and EMCV, respectively. At 1h after infection, medium was removed and replaced with DMEM containing 10 % FCS and the cells were incubated for 2 days at 37 °C. Then the supernatants were collected and centrifuged at 3,000 rpm for 15 min to remove cells for avoiding cellular RNA contamination. Then the supernatants were harvested and centrifuged at 25,000 rpm for 90 min in an SW28 rotor at 4 °C. The viral pellet was suspended in TRIzol reagent (Invitrogen) and RNA was extracted. 5-10 µg/ml VSV RNA and 0.5-3 µg/ml EMCV RNA were obtained from single preparation.

#### Analysis of total protein synthesis.

Cultures of wild-type and *MDA5*<sup>-/-</sup> MEFs were infected with EMCV. At various time of labeled by incorporation of 50  $\mu$ Ci of [<sup>35</sup>S]Met-Cys (GE Healthcare) for 1 h. Then the cells were lysed in a lysis buffer containing 1.0% Nonidet-P40, 150 mM NaCl, 20 mM Tris-Cl (pH7.5), 1 mM EDTA and protease inhibitor cocktail (Roche). Total cell extracts were separated by polyacrylamide gel electrophoresis, and the proteins were visualized by autoradiography.

1. Martin, L. R., Neal, Z. C., McBride, M. S. & Palmenberg, A. C. Mengovirus and encephalomyocarditis virus poly(C) tract lengths can affect virus growth in murine cell culture. *J Virol* 74, 3074-81 (2000).
2. Shin, T. & Koh, C. S. Immunohistochemical detection of osteopontin in the spinal cords of mice with Theiler's murine encephalomyelitis virus-induced demyelinating disease. *Neurosci Lett* 356, 72-4 (2004).

## II. Supplemental Figure Legends

### Supplementary Fig. 1: Targeted disruption of the murine *MDA5* gene.

(a) Structure of the mouse *MDA5* gene, the targeting vector and the predicted disrupted gene. Closed boxes denote the coding exon. B; BamH I (b) Southern blot analysis of offspring from the heterozygote intercrosses. Genomic DNA was extracted from mouse tails, digested with BamHI, separated by electrophoresis and hybridized with the radiolabelled probe indicated in (a). Southern blot gave a single 9.4 kb band for wild-type (+/+), a 4.6 kb band for homozygous (-/-) and both bands for heterozygous (+/-) mice. (c) Northern blot analysis of peritoneal exudates cells (PECs). Total RNA from wild-type (WT) and *MDA5*<sup>-/-</sup> PECs treated with 1000 U/ml IFN- $\beta$  for 8 h was extracted and subjected to Northern blot analysis for the expression of *MDA5* mRNA. The same

membrane was rehybridized with a  $\beta$ -actin probe. (d) Western blot analysis of MDA5 expression. WT and MDA5<sup>-/-</sup> MEFs were treated with 1000 U/ml IFN- $\beta$  for 8 h, and whole cell lysates were immunoblotted with antibody against MDA5. N.S. non specific.

**Supplementary Fig. 2: Involvement of MDA5 or RIG-I in the recognition of dsRNAs.**

- (a) RIG-I<sup>-/-</sup> and MDA5<sup>-/-</sup>, and their littermate WT mice were injected intravenously with 200  $\mu$ g of poly I:C for the indicated periods and the production of IFN- $\beta$  in the sera was measured by ELISA. The data are means  $\pm$  S.D. of sera samples.
- (b) GMCSF-DCs from RIG-I<sup>-/-</sup> and MDA5<sup>-/-</sup>, TRIF<sup>-/-</sup> and their littermate control mice were incubated in the presence of 50, 250  $\mu$ g/ml poly I:C for 24 h. The production of IFN- $\alpha$  in the culture supernatants was measured by ELISA.
- (c) Generation of different lengths of dsRNAs corresponding to mouse lamin A/C. Different lengths of dsRNAs corresponding to mouse lamin A/C were synthesized as described in Methods section. 1  $\mu$ g of dsRNAs were separated on 1% Agarose gel and visualized by staining with ethidium bromide. All dsRNAs synthesized appear with the estimated size.

**Supplementary Fig. 3: Contribution of RIG-I and MDA5 in the induction of genes encoding type I IFNs and IFN-inducible proteins in response to viral infection.**

- (a) WT, RIG-I<sup>-/-</sup> or MDA5<sup>-/-</sup> MEFs were treated with 5  $\mu$ g/ml poly I:C complexed with lipofectamine 2000 for the indicated periods. Total RNA was extracted and subjected to the Northern blot analysis for the expression of IFN- $\beta$ , IP10 and  $\beta$ -actin mRNA.
- (b) WT, RIG-I<sup>-/-</sup> and MDA5<sup>-/-</sup> MEFs were treated with 5  $\mu$ g/ml dsRNA corresponding to Lamin A/C (600 bps) complexed with lipofectamine 2000 for the indicated periods. Total RNA was extracted and subjected to the Northern blot analysis for the expression of